Targeting Calcium Signaling To Induce Epigenetic Reactivation of Tumor Suppressor Genes in Cancer

Noël J.-M. Raynal[1,2], Justin T. Lee[1], Youjun Wang[3], Annie Beaudry[2], Priyanka Madireddi[1], Judith Garriga[1], Gabriel Malouf[4*], Sarah Dumont[4], Elisha J. Dettman[4], Vazganush Gharibyan[4], Saira Ahmed[4], Woonbok Chung[1], Wayne E. Childers[5], Magid Abou-Gharbia[5], Ryan A. Henry[6], Andrew J. Andrews[6], Jaroslav Jelinek[1], Ying Cui[7], Stephen B. Baylin[7], Donald L. Gill[8], and Jean-Pierre J. Issa[1]

[1]Fels Institute for Cancer Research and Molecular Biology, Temple University School of Medicine, 3307 North Broad Street, Philadelphia, PA, 19140, USA. [2]Département de pharmacologie, Université de Montréal and Sainte-Justine University Hospital Research Center, 3175 Chemin de la Côte Sainte-Catherine, Montréal (QC), Canada, H3T1C5. [3]Beijing Key Laboratory of Gene Resources and Molecular Development College of Life Sciences, Beijing Normal University, Beijing 100875, P.R. China. [4]Department of Leukemia, The University of Texas MD Anderson Cancer Center, 1515 Holcombe Blvd., Houston, TX, 77030, USA. [5]Moulder Center for Drug Discovery Research, 3307 North Broad Street, Philadelphia, PA, 19140, USA. [6]Department of Cancer Biology, Fox Chase Cancer Center, 333 Cottman Avenue, Philadelphia, PA, 19111, USA. [7]The Sidney Kimmel Comprehensive Cancer Center at Johns Hopkins 401 North Broadway, Baltimore, MD 21231, USA. [8]Department of Cellular and Molecular Physiology, The Pennsylvania State University College of Medicine, The Milton S. Hershey Medical Center, 500 University Drive, Hershey, PA 17033-0850.

Corresponding Author: Jean-Pierre J. Issa, Fels Institute for Cancer Research and Molecular Biology, Temple University School of Medicine, 3307 North Broad Street, Philadelphia, PA, 19140, USA. jpissa@temple.edu

*Current Address

Gabriel Malouf

Hôpital de la Pitié-Salpétrière

Medical Oncology

Paris, France

Running title: Targeting Calcium Signaling Produces Epigenetic Reactivation

Disclosure of Potential Conflicts of Interest: No potential conflicts of interest were disclosed.

Grant Support: Dr J-P Issa is an American Cancer Society Clinical Research professor supported by a generous gift from the F. M. Kirby Foundation. This work was supported by NIH grants CA100632 and CA046939 (J-P Issa).

Abstract

Targeting epigenetic pathways is a promising approach for cancer therapy. Here, we report on the unexpected finding that targeting calcium signaling can reverse epigenetic silencing of tumor suppressor genes (TSGs). In a screen for drugs that reactivate silenced gene expression in colon cancer cells, we found three classical epigenetic targeted drugs (DNA methylation and histone deacetylase inhibitors) and 11 other drugs that induce methylated and silenced CpG island promoters driving a reporter gene (GFP) as well as endogenous TSGs in multiple cancer cell lines. These newly identified drugs, most prominently cardiac glycosides, did not change DNA methylation locally or histone modifications globally. Instead, all 11 drugs altered calcium signaling and triggered calcium-calmodulin kinase (CamK) activity leading to MeCP2 nuclear exclusion. Blocking CamK activity abolished gene reactivation and cancer cell killing by these drugs, showing that triggering calcium fluxes is an essential component of their epigenetic mechanism of action. Our data identify calcium signaling as a new pathway that can be targeted to reactivate TSGs in cancer.

Introduction

In cancer, the epigenome is aberrantly reprogrammed leading to a wide range of heritable changes in gene expression such as silencing of tumor suppressor genes (TSG) (1). The most studied epigenetic aberrations in cancer involve DNA methylation and histone post-translational modifications. Acquisition of *de novo* methylation in cytosine of CpG dinucleotide at the promoter region of TSG results in stable gene silencing through direct inhibition of transcription factor binding or by recruitment of methyl-binding domain (MBD) proteins such as MeCP2 (1,2). These MBDs are associated with other repressor complexes including histone deacetylases (HDAC) that are responsible for global loss of histone acetylation resulting in gene silencing and heterochromatin formation (2).

Since these epigenetic modifications are reversible, one goal of epigenetic therapy of cancer is to reverse these alterations and induce TSG reactivation leading to cancer cell differentiation and cancer cell death (3). Clinical efficacy of epigenetic drugs led to their approval for the treatment of hematological malignancies and occasional proof-of-principle responses can be seen in solid tumors (2,4). However, treatment options are limited to a small number of epigenetic drugs approved in the clinic with two DNA methylation inhibitors (decitabine and azacitidine) and two HDAC inhibitors (vorinostat and depsipeptide). There is a need to discover new candidate epigenetic drugs, including some that work through other mechanisms of action. Drug discovery initiatives are underway in rare and specific cancer types with well-defined mutations in epigenetic effectors. However, these efforts may take years before approval and may have limited effects outside of a restricted patient population (5).

In order to discover new epigenetic drugs that can be rapidly tested in the clinic, we performed an unbiased epigenetic drug screen using US-FDA approved drug libraries. The rationale is that positive hits can be rapidly repositioned for cancer treatment because these drugs have known safety, pharmacodynamics and pharmacokinetics (6). As a platform for epigenetic drug screening, we used the well-characterized YB5 cell-based system which is derived from the human colon cancer cell line, SW48 (7,8). YB5 cells contain a single insertion of cytomegalovirus (*CMV*) promoter driving green fluorescent protein (*GFP*) gene. GFP expression is silenced in >99.9% of YB5 cells by epigenetic mechanisms because its *CMV* promoter has DNA hypermethylation and is embedded in repressive chromatin with histone deacetylation and histone methylation marks (Fig. 1A) (7). In YB5 cells, *GFP* behaves similarly to endogenous TSGs silenced by epigenetic mechanisms and it can be reactivated by treatment with DNA methylation inhibitors and/or HDAC inhibitors (7,8). We previously demonstrated that GFP reactivation induced by decitabine is characterized by both DNA demethylation and chromatin resetting at the *CMV* promoter region (7). Moreover, we also showed that HDAC inhibitors induced GFP reactivation through chromatin resetting at the *CMV* promoter with an increase in histone acetylation without any changes in DNA methylation (8). Since the goal of the epigenetic therapy is to reactivate silenced TSGs, we used the YB5 system as a cell-based assay for epigenetic drug screening.

Here, our screen revealed a new mechanism where targeting calcium signaling can reactivate TSGs silenced by epigenetic mechanism in cancer cells. The alteration in calcium signaling results in activated calcium-calmodulin kinase which played a central role in TSGs reactivation and cancer cell killing.

Materials and Methods

Cell culture

Human colon cancer cell line YB5 and its parental cell line SW48 cell line were cultured in L-15 medium. Human colon cancer cell line HCT116 was cultured in McCoy medium. In HCT116 human colon cancer cells, *GFP* sequence was inserted in exon 2 of the TSG secreted frizzled related protein 1 (*SFRP1*) making the HCT116 *SFRP1-GFP* cell line. This locus is silenced by promoter DNA hypermethylation in HCT116 (9). GFP expression detected by flow cytometry corresponded to the activity of *SFRP1* promoter and was measured in less than 10% of the cells. Normal colon cells, CRL-1831, were grown in DMEM F-12 medium supplement with 10 ng/ml cholera toxin, 0.005 mg/ml insulin, 0.005 mg/ml transferrin, 100 ng/ml hydrocortisone, and 100 mM HEPES. Leukemia cell lines, K562 and HL-60 were cultured in RPMI-1640. HEK293T were grown in DMEM. All cell culture media were supplemented with 10% fetal bovine serum. Colon cancer and leukemic cells were grown in log phase in 1% and 5% CO_2 atmosphere, respectively. SW48, K562 and HL-60 cell lines were obtained from American Type Culture Collection (2005-2007) and were authenticated at MD Anderson Cancer Center genomic core facility by DNA fingerprinting in 2011. CRL-1831 cell line was obtained from American Type Culture Collection in 2012 and used within two months from the purchase. HCT116 and HEK293T were obtained from the Baylin and Gill labs and were genetically engineered cell lines that were not further authenticated.

Drugs and treatments

Drug libraries of FDA-approved drugs were obtained from NCI-Developmental Therapeutics Program (Combo Plate 3948/99 containing 77 drugs, NCI Oncology Drug set 4640/34 containing 52 drugs, NCI Oncology Drug set 4641/34 with 37 drugs) and from commercially available US Drug collection library with 1040 drugs (MS Discovery). A total of 1118 unique FDA-approved drugs were screened. Log-phase growing YB5 cells were treated with drug libraries ($n \geq 1$) with two different schedules. The first schedule consisted of a 72h treatment at 10 μM where drugs and media were replaced every day. Cells were incubated an additional 24h without drugs before analysis. This schedule was designed to discover putative new hypomethylating agents since the induction of DNA demethylation may require several cell divisions to become detectable (2). The second schedule consisted of a 24h treatment at 50 μM. Cells were immediately analyzed after the treatment. This schedule was designed to discover drugs that would reactivate GFP by chromatin remodeling since, in this cell line, HDAC inhibitors can reactivate GFP in 24h without any changes in DNA methylation at the *CMV* promoter. For validation purposes and pharmacologic (leptomycin L2913) modulation, drugs were purchased at Sigma-Aldrich and dissolved either in DMSO, ethanol or sterile PBS according to the manufacturers recommendations and stocks were kept frozen in -80ºC. CamK inhibitors were purchase at EMD Millipore (Kn-93, 422712, and Kn-92, 422709).

Flow cytometry

After treatment, cells were trypsinized and resuspended in cell culture media with propidium iodide (PI) to stain dead cells. For epigenetic drug screening with YB5 cells, GFP and PI fluorescence were measured using BD LSR II flow cytometer. Validations

were performed using Millipore Guava flow cytometer with YB5 or *SFRP1-GFP* HCT116 cells. Flow cytometry analysis was also used prior to any type of extractions (RNA, DNA, and proteins) to ensure a similar level of GFP reactivation following drug treatments for each biological replicate. Flow cytometry results were plotted as GFP fluorescence on the X-axis and PI on the Y-axis (Supplementary Fig. S1A-D). Positive hits were designated using two selection criteria. Firstly, we excluded all autofluorescent drugs (like antimalarials) because autofluorescence creates a false positive signal that bleaches into GFP channel. Drugs that showed more than 8% of the cells in the double positive quadrant were discarded. This threshold value was calculated as the sum of the average plus one standard deviation of the percentage of cells detected in the double positive quadrant in the entire screen data set. Secondly, the lowest detection threshold for GFP reactivation was set at 2.2% of the cells present in the GFP positive quadrant. This value was established experimentally and corresponded to the lowest GFP value obtained in the screen that was confirmed during our validation step with drugs purchased from independent suppliers.

RNA extraction, cDNA synthesis, quantitative real-time PCR

Total RNA (2 μg) was extracted using Trizol (Invitrogen) and cDNA was synthesized using High-Capacity cDNA Kit (Applied Biosystems). Quantification of cDNA was done by qPCR with the Universal PCR Master Mix (Bio-Rad) using ABI Prism 7900HT system. Results were obtained from at least three independent experiments where each sample was analyzed in triplicate. 18S was used as a reference gene. All primers have been described previously (7,8).

DNA extraction and DNA methylation analysis

DNA extraction, bisulfite conversion and pyrosequencing were carried out as previously described (7,8).

Histone extraction and Western blots

For acid histone extraction, cells were harvested and washed twice with ice-cold PBS supplemented with 10 mM sodium butyrate to retain levels of histone acetylation. Cell pellets were resuspended cells in Triton Extraction Buffer (TEB: PBS containing 0.5% Triton X 100 (v/v), 2 mM phenylmethylsulfonyl fluoride (PMSF), 0.02% (w/v) NaN3, complete protease inhibitor cocktail, 10 mM sodium butyrate). Cell lysis was induced after 10 minutes incubation on ice with gentle stirring. Lysates were centrifuged at 6,500 g for 10 minutes at 4°C. Supernatant was discarded. Cells were washed in half the volume of TEB and centrifuged as before. Pellets were resuspended in 0.2N HCl. Histones were acid extracted over night at 4°C. Samples were centrifuged at 6,500 g for 10 minutes at 4°C. Histone proteins contained in the supernatant were saved and protein concentration was determined using the Bradford assay. Extracted histones were stored at -80°C. Histone extracts were run in 12% SDS-PAGE precast gels (Bio-Rad, 345-0118). Proteins were transferred to PVDF membranes in 10mM CAPS (pH 11) containing 10% methanol and detected by using specific primary antibodies and horseradish peroxidase-conjugated secondary antibodies (GE) and Enhanced Chemiluminescence reagent (Pierce). PVDF membranes were incubated with specific primary antibodies. Commercially available antibodies were purchased for H3K4-3me (Active motif, 39159),

H3K9-3me (ABCAM, AB 8898), H3K14-Ac (Active motif, 39697), H3K9-Ac (Active motif, 39917), H3K27-3me (Active motif, 39155), H3K27-Ac (Upstate, 07360), and H3 (Active motif, 39763), MeCP2 (ABCAM, AB2828).

Statistical analysis

Differences between groups were assessed using a one-way ANOVA. The *P* value was evaluated by the Tukey–Kramer Multiple Comparison Test. Statistics and graphical representations were performed using GraphPad Prism® software.

Results

Epigenetic drug screening and positive hits validation

We screened over 1,100 US-FDA approved drugs obtained from the NCI and commercial sources using two dose-schedules (Fig. 1B). The first schedule (10 μM, for 72h followed by 24h without drug) was designed to discover epigenetic drugs that require several cell cycles to induce robust gene reactivation, as observed with DNA methylation inhibitors. This schedule induced significant DNA demethylation and was associated with gene reactivation in YB5 cells (7). The second schedule (50 μM, for 24h) was selected to discover epigenetic drugs that produce rapid gene reactivation, as seen with HDAC inhibitors. Based on the very low background in the YB5 system (less than 0.1% of the cells express detectable levels of GFP) (Supplementary Fig. S1A) and activity seen in negative controls, positive hits in the screen were defined as those non-auto-fluorescent drugs inducing more than 2.2% of GFP+ cells (Supplementary Fig. S1B-E).

The drug screen revealed 23 (2%) and 77 (7%) positive hits at 10 μM (for 72h) and at 50 μM (for 24h) respectively, while 12 drugs (1%) were identified in both schedules (Fig. 1C-E). The highest inducers of GFP expression were the DNA methylation inhibitors decitabine (at 10 μM, for 72h) and azacitidine (at 50 μM, for 24h) producing respectively 30% and 16% GFP+ cells (Supplementary Table S1 and S2). Azacitidine induced GFP-reactivation after a short treatment of 24h which can be explained by the number of YB5 cells in S phase during the treatment (2). The HDAC inhibitor vorinostat was also identified in this screen producing 2.6% GFP+ cells (Supplementary Table S2). Thus, all three known epigenetic drugs represented in the libraries were rediscovered in this blinded screen, validating the approach.

Because of the unexpected large number of positive hits, we focused on the 12 drugs identified in both dose-schedules (Fig. 1E). For validation, compounds were purchased from separate suppliers and tested for GFP reactivation in YB5 cells. Of these 12 hits, all except tilmicosin (which was low positive) were validated. These 11 validated drugs fell into 3 groups (Fig. 1F). The first one included the known epigenetic drugs decitabine, azacitidine, and vorinostat. The second group encompassed cardiac glycosides such as ouabain, lanatoside C, digoxin, digitoxin, and proscillaridin A. All cardiac glycosides represented in the libraries reactivated GFP suggesting a drug class effect. The last group was labeled as antibiotics/others and contained oxyquinoline (antibiotic), disulfiram (a drug used for alcoholism treatment), and arsenic trioxide (anticancer drug) (Fig. 1F). In the validation studies, GFP reactivation was tested at multiple doses (Fig. 2A-F). All cardiac glycosides induced dose-dependent GFP reactivation in the nanomolar range at clinically relevant concentrations, with proscillaridin A being the most potent

(Supplementary Fig. S2A-B). We also validated 3 additional antibiotics (pyrithion zinc, cycloheximide, and thiram) in the antibiotic/others sub-group that were identified in the screen at 50 μM only but were positive during the validation using both schedules. Therefore, we validated a total of 14 FDA-approved drugs encompassing three well-known epigenetic drugs and 11 candidate epigenetic drugs.

No changes in classical epigenetic pathways

We confirmed *GFP* mRNA reactivation after 24h treatment by qPCR (Fig. 3A). We also detected gene reactivation in 3 endogenous TSGs silenced by epigenetic mechanism in YB5 cells (*CDH13*, *RIL*, *TIMP-3*) as well as the stress response gene *P21* (*CDKN1A*) (Supplementary Fig. S3A-D). In addition, we measured *SFRP1* reactivation, another DNA hypermethylated TSG in HCT116 colon cancer cells (9,10). In this cell line, *GFP* sequence was inserted in exon 2 of *SFRP1* making its activation detectable by flow cytometry (9). Similarly to YB5 cells, all drugs reactivated *SFRP1* gene the HCT116 *SFRP1-GFP* system (Fig. 3B). To identify a mechanism of action, we asked whether candidate epigenetic drugs induced gene reactivation through known epigenetic mechanism such as DNA demethylation or histone acetylation. First, we measured DNA methylation locally in the promoter regions of reactivated genes (*CMV* and endogenous TSGs) and at *LINE-1* repeats to assess global DNA methylation levels. Using bisulfite pyrosequencing assays designed in the promoter regions close to the transcription start site (8), we found that none of the drugs reduced DNA methylation at the *CMV* (Fig. 3C) or *TIMP-3* (Supplementary Fig. S4A) promoters or globally at *LINE-1* repeats (Fig. 3D), except for decitabine (a well-known hypomethylating drug). We then measured

quantitatively histone acetylation levels by mass-spectrometry on 9 residues in histone 3 (H3) and histone 4 (H4). No significant changes were observed, except with vorinostat, a well-known HDAC inhibitor which increased histone acetylation levels on lysine 9, 14, 18 and 23 of histone 3 and on lysine 8, 12 and 16 of histone H4 (Fig. 3E and Supplementary Fig. S4B). A similar lack of global effects was observed by Western blots for histone activating marks (H3K4-me3, H3K9-ac, and H3K27-ac) or histone inactivating marks (H3K9-me3 and H3K27-me3) (Supplementary Fig. S4C).

Intracellular Ca^{2+} fluxes induced by newly identified drugs

Since neither DNA demethylation nor global chromatin modifications explained TSG reactivation by the newly identified drugs, we searched for alternative mechanisms. Surprisingly, when searching for a mechanism of action of the newly identified drugs, we noted that most of them (9 out of 11) drugs are known to increase intracellular calcium (Ca^{2+}) levels (11-14). No data were found regarding the three known epigenetic drugs and calcium signaling. Interestingly, it was reported in neurons that cytosolic increase in Ca^{2+} levels activate Ca^{2+}-calmodulin kinase (CamK) which release the methyl-binding protein, MeCP2 from silenced promoters, leading to gene reactivation (15,16).

To test whether this mechanism could explain TSGs reactivation in cancer cells by the newly identified drugs, we first characterized Ca^{2+} channels in YB5 cells. Using Ca^{2+} sensitive dye (fura-2), we determined that YB5 cells do not express functional L-type voltage operated Ca^{2+} channels (Supplementary Fig. S5A-B). Instead, YB5 cells have functional plasma membrane store operated Ca^{2+} entry (SOCe) channels which transports extracellular Ca^{2+} into the cytosol in response to a decrease in Ca^{2+} level in the

endoplasmic reticulum (ER) store. The activity of these plasma membrane channels was demonstrated by the effect of SOCe inhibitors reducing cytosolic Ca^{2+} entry triggered by the ER Ca^{2+} pump blocker, thapsigargin (Supplementary Fig. S5C) (17,18).

Then, we characterized the effects of drug treatments in YB5 cells on cytosolic Ca^{2+} levels at rest, ER Ca^{2+} levels and SOCe activity in response to Ca^{2+} ionophore, ionomycin or thapsigargin followed by the addition of 1 mM Ca^{2+} in the media (a cation-safe solution). Interestingly, known epigenetic drugs did not alter Ca^{2+} homeostasis (Fig. 4A). However, cardiac glycosides and arsenic trioxide reduced ER Ca^{2+} levels (1^{st} peak) while strongly inhibiting SOCe mediated Ca^{2+} entry (2^{nd} peak) (Fig. 4B and Supplementary Fig. S5D). Even though, ER Ca^{2+} levels were significantly reduced, we could not measure an increase in cytosolic Ca^{2+} suggesting a transient spark in cytosolic Ca^{2+} after treatment with digitalis compounds (19). In another model of HEK293 cells expressing the genetically-encoded calcium sensors (D1ER cameleon system) specifically expressed in the ER, we confirmed digitoxin-induced reduction in ER Ca^{2+} (Supplementary Fig. S5E) (20). Finally, we could detect an increased cytosolic Ca^{2+} level (higher baseline Ca^{2+} signal) after only pyrithion zinc treatment while both pyrithion zinc and disulfiram increased Ca^{2+} levels in the ER (1^{st} peak) (Fig. 4C). Thus, most of the candidate epigenetic drugs induce measurable intracellular Ca^{2+} changes in YB5 cells by different mechanisms of action which result in cytosolic Ca^{2+} sparks or sustained increased levels. It is noteworthy that cardiac glycosides are well-known Na^+/K^+-ATPase pump blockers used in heart failure treatment (11). To assess the impact of Na^+/K^+-ATPase pump inhibition on GFP reactivation in YB5 cells, we treated YB5 cells with orthovanadate, an inorganic Na^+/K^+-ATPase inhibitor and did not detect GFP reactivation. These data

suggest that the epigenetic activity of cardiac glycosides might be independent of Na^+/K^+-ATPase (data not shown).

We further explored the mechanism of SOCe inhibition induced by cardiac glycosides. Store operated Ca^{2+} entry (SOCe) is mediated by the highly Ca^{2+}-selective Orai1 channels which are activated by STIM proteins in response to a decrease in ER Ca^{2+} levels. STIM translocates into ER-plasma membrane junctions to tether and activate Orai1 channels (21,22). For these experiments, we used a well-established model of HEK293 cells overexpressing Orai1-CFP and STIM1-YFP (23). We found that digitoxin did not affect STIM1-Orai1 coupling as maximal FRET signal between STIM1 and Orai1, obtained after ionomycin treatment, was unaltered by digitoxin (Supplementary Fig. S5F). Wild-type and overexpressing STIM1-Orai1 HEK293 cells showed similar inhibition of SOCe and reduction in ER Ca^{2+} size by digitoxin (Fig. 4D and Supplementary Fig. S5G). Importantly, these effects on Ca^{2+} levels were not caused by changes in cytosolic pH (Supplementary Fig. S5H) (20,24,25). Finally, digitoxin specifically inhibited Ca^{2+} influx through Orai1 in HEK293 cells expressing either constitutively active STIM1 mutant (STIM1D76A) or constitutively active Orai1 mutant (O1-V102C) (Fig. 4E-F) (26). In these experiments, we used the antihistamine fexofenadine as a control for specificity of action since this drug treatment does not induce GFP reactivation. Together, the data demonstrate that cardiac glycosides altered Ca^{2+} levels by causing potent SOCe inhibition.

Ca^{2+} signaling through CamK is essential for gene reactivation

Calcium/calmodulin-dependent protein kinase (CamK), a multifunctional serine/threonine kinase, is a central molecule which is activated by an increase in cytosolic Ca^{2+} leading to gene expression changes in part caused by the unbinding of chromatin repressors such as the methyl-binding protein, MeCP2 from their silenced promoters (15,27-29). Except for known epigenetic drugs, all candidate epigenetic drugs induce intracellular Ca^{2+} changes. Thus, we tested the role of CamK in YB5 cells treated with known and candidate epigenetic drugs. Drug-induced reactivation of *GFP* and endogenous TSGs (*TIMP-3* and *WIF-1*) was significantly reduced by pharmacologic inhibition of CamKII using Kn-93 while Kn-92, its weaker analogue, had a much smaller effect (Fig. 5A and Supplementary Fig. S6A-B) (30). As expected, GFP expression induced by azacitidine was not sensitive to Kn-93 inhibition since this hypomethylating drug did not alter Ca^{2+} fluxes (Fig. 5A).

We next hypothesized that the epigenetic effects of CamK activation by Ca^{2+} signaling relate to unbinding of MeCP2 from repressed promoters, as previously reported in normal neuronal cells (15,16,28,29). Using ChIP-qPCR following cardiac glycoside treatment (Lanatoside C), we found that MeCP2 occupancy was reduced at several DNA hypermethylated promoters (Supplementary Fig. S7), suggesting that drug-induced dissociation of MeCP2 binding is associated with gene reactivation. Most interestingly, using confocal microscopy, we observed nuclear versus cytoplasmic redistribution of MeCP2 after proscillaridin treatment (Fig. 5B). Following 24h and 48h treatment with proscillaridin at 500 nM, MeCP2 staining was enriched in the cytoplasm in most of the cells (Fig. 5B). In untreated cells, MeCP2 staining was mainly concentrated in the nucleus and a weak signal was detected in the cytoplasm as already observed by others

(31). MeCP2 antibody specificity was verified by using siRNA (in western blot experiments and confocal microscopy on YB5 untreated and treated with proscillaridin A) and HEK293T cells overexpressing MeCP2 (Supplemental Fig. S8-S9). Finally, we showed that these effects of the positive hits identified in the screen may relate to export of regulatory proteins from the nucleus to the cytoplasm. Blocking the exportin pathway of protein transport from the nucleus to the cytoplasm by leptomycin significantly reduced drug-induced GFP reactivation in YB5 cells (Supplementary Fig. S10).

Since CamKII appeared to mediate gene reactivation, we next tested whether the selective cancer cell killing was also CamKII-dependent. Percentages of apoptotic cells, viable cells and dead cells were measured in colon cancer (SW48 – YB5 parent cell line) and leukemia (K562 and HL-60) cell lines following 48h drug treatment alone or in combination with CamKII inhibitor, Kn-93 and its less active derivative, Kn-92. For all cell lines, drugs significantly induced cytotoxicity while, as expected for this brief treatment period, hypomethylating drugs did not. Kn-93 rescued almost completely the drug-induced toxic effects (Fig. 5C, and Supplementary Fig. S11, S12 and S13). These data suggest that CamK activation is a key effector of the anticancer activity of these FDA-approved drugs.

Anticancer activity and cancer selectivity

We next assessed the anticancer activity of the newly identified candidate epigenetic drugs in YB5 cells. Anchorage-dependent colony formation assays were performed for long-term cytotoxicity evaluation. All drugs reduced cancer cell survival in a dose and time dependent manner (Fig. 6A-C). Anticancer activity was stronger for the newly

identified drugs compared to known epigenetic drugs. Anchorage-independent colony assays were then performed by gauging colony formation in soft agar. All drugs produced a significant dose-dependent reduction in the number of colonies; with proscillaridin A being the most potent (Fig. 6D). To address the question of cancer cell selectivity, we compared the viability of normal colon cells (CRL-1831) versus colon cancer cells (SW48). We used YB5's parental cell line SW48 for this because GFP expression could affect viability measurements performed by flow cytometry. After 48h treatment at doses producing the strongest GFP reactivation in YB5 cells, cell viability was reduced in cancer cells but not in normal cells (Fig. 6E) demonstrating the cancer selectivity of these drugs.

Discussion

There is a need to discover new epigenetic targets and drugs to induce TSG reactivation in cancer cells. The arsenal of epigenetic drugs approved in the clinic is currently limited to only four drugs targeting only two separate mechanisms. Based on the high number of epigenetic targets in cancer, there is a great interest in discovering new targets that can be used to reactivate TSGs and reprogram cancer cells to eradicate their clonogenic potential and induce their differentiation. We used our live cell-based assay where we measured GFP reactivation as surrogate for TSG reactivation. Overall, we identified 14 hits including 3 well-known epigenetic drugs and 11 other FDA-approved drugs encompassing cardiac glycosides and some antibiotics.

To identify the mechanism responsible for GFP and endogenous TSGs reactivation, we first analyzed promoter DNA methylation and histone modifications. No changes were detected after treatment with the cardiac glycosides or the antibiotics while TSGs reactivation was detected. Surprisingly, we noticed that most of the newly identified drugs are known to induce alterations in Ca^{2+} signaling in normal cells. We demonstrated that these changes in Ca^{2+} signaling also occurred in our cancer cell screening system (YB5 cells) and only after treatment with the newly epigenetic drugs but not with well-known epigenetic drugs such as DNA methylation and HDAC inhibitors. This difference suggested a separate mechanism of action. Our data showed that reactivation of endogenous epigenetically silenced TSGs was linked to Ca^{2+} signaling and CamK activation. Mechanistically, our data suggest that gene reactivation may involve gene derepression by inducing MeCP2 eviction from repressed promoters to the cytoplasm

through the exportin pathway (Supplementary Fig. S14). Interestingly, the anticancer activity could also be modulated by CamK pharmacological inhibition.

Consistent with our work**,** other studies have demonstrated a CamK-dependent mechanism producing MeCP2 release from silenced promoters leading to gene reactivation (15,28,29). Interestingly, our data further demonstrate redistribution of MeCP2 to the cytoplasm after drug-induced CamK activation. The relationship between MeCP2 binding to methylated-CpGs and Ca^{2+} has been described in neurons where MeCP2 phosphorylation is involved in intracellular localization during neuronal differentiation (31,32). Phosphorylation sites of MeCP2 are known to modify its binding to other epigenetic cofactors but more studies are needed to clearly understand the role of CamK and MeCP2 phosphorylation sites. Nevertheless, our study shows that the CamK-MeCP2 interaction previously linked only to differentiation can be exploited against cancer cells to reactivate silenced TSG. These data also demonstrate a key role for calcium fluxes in epigenetic silencing in neoplasia.

Interestingly, we identified a class effect for the cardiac glycoside subgroup where all these heart failure drugs present in the libraries scored positive in the screen and also separately validated. These drugs are relevant for cancer treatment since epidemiologic studies have shown that patients treated with cardiac glycosides for heart failure exhibit a reduced cancer rate and less aggressive cancers (11,33,34). Moreover, in vitro studies have previously shown selective cancer killing for some of these cardiac glycosides which we now relate to Ca^{2+} signaling and TSGs reactivation (35). Our data suggest that their chemopreventive or chemotherapeutic activity may be in part due to their ability to target Ca^{2+} fluxes and reactivate epigenetically silenced TSGs. Another drug we

identified as having effects on gene silencing is arsenic trioxide which has marked activity in acute promyelocytic leukemia (36), a disease characterized by a block in cell differentiation (37). Our data suggest that epigenetic modulation may be part of its anti-neoplastic mechanism of action. Interestingly, cytotoxic drugs or targeted drugs (e.g. tyrosine kinase inhibitors) used in cancer chemotherapy did not reactivate GFP, pointing to the specificity of the identified hits. This was verified separately from the screen for many cytotoxic drugs (38). Thus, the mechanism of action of the positive hits is likely to be specific disruption of epigenetic pathways involved in gene silencing rather than non-specific effects seen with many anti-proliferatives.

Finally, it is worth noting that Ca^{2+} signaling is essential to initiating epigenetic reprogramming in early embryogenesis (39) and our data extend these findings to cancer therapy. Also, the mechanism of epigenetic action of these drugs is unlikely to be traced to a single chromatin regulator; rather, Ca^{2+} signaling through CamK activation may have effects on multiple epigenetic acting proteins simultaneously. It will be interesting to determine what targets, other than MeCP2, might be phosphorylated by CamK activation.

In summary, our data identify Ca^{2+} signaling as a new pathway that can be targeted to reactivate TSGs in cancer. This study suggest that cardiac glycosides and other FDA-approved drugs such as some antibiotics represent interesting drugs for cancer epigenetic chemotherapy aiming to reactivate epigenetically silenced TSGs.

References

1. Kelly TK, De Carvalho DD, Jones PA. Epigenetic modifications as therapeutic targets. Nat Biotechnol 2010;28(10):1069-78.
2. Taby R, Issa JP. Cancer epigenetics. CA Cancer J Clin 2010;60(6):376-92.
3. Baylin SB, Jones PA. A decade of exploring the cancer epigenome - biological and translational implications. Nature reviews Cancer 2011;11(10):726-34.
4. Juergens RA, Wrangle J, Vendetti FP, Murphy SC, Zhao M, Coleman B, et al. Combination epigenetic therapy has efficacy in patients with refractory advanced non-small cell lung cancer. Cancer discovery 2011;1(7):598-607.
5. Arrowsmith CH, Bountra C, Fish PV, Lee K, Schapira M. Epigenetic protein families: a new frontier for drug discovery. Nature reviews Drug discovery 2012;11(5):384-400.
6. Tailler M, Senovilla L, Lainey E, Thepot S, Metivier D, Sebert M, et al. Antineoplastic activity of ouabain and pyrithione zinc in acute myeloid leukemia. Oncogene 2012;31(30):3536-46.
7. Si J, Boumber YA, Shu J, Qin T, Ahmed S, He R, et al. Chromatin remodeling is required for gene reactivation after decitabine-mediated DNA hypomethylation. Cancer research 2010;70(17):6968-77.
8. Raynal NJ, Si J, Taby RF, Gharibyan V, Ahmed S, Jelinek J, et al. DNA methylation does not stably lock gene expression but instead serves as a molecular mark for gene silencing memory. Cancer research 2012;72(5):1170-81.
9. Cui Y, Hausheer F, Beaty R, Zahnow C, Issa JP, Bunz F, et al. A recombinant reporter system for monitoring reactivation of an endogenously DNA hypermethylated gene. Cancer research 2014;74(14):3834-43.
10. Suzuki H, Gabrielson E, Chen W, Anbazhagan R, van Engeland M, Weijenberg MP, et al. A genomic screen for genes upregulated by demethylation and histone deacetylase inhibition in human colorectal cancer. Nature genetics 2002;31(2):141-9.
11. Prassas I, Diamandis EP. Novel therapeutic applications of cardiac glycosides. Nature reviews Drug discovery 2008;7(11):926-35.
12. Sook Han M, Shin KJ, Kim YH, Kim SH, Lee T, Kim E, et al. Thiram and ziram stimulate non-selective cation channel and induce apoptosis in PC12 cells. Neurotoxicology 2003;24(3):425-34.
13. Jatoe SD, Lauriault V, McGirr LG, O'Brien PJ. The toxicity of disulphides to isolated hepatocytes and mitochondria. Drug Metabol Drug Interact 1988;6(3-4):395-412.
14. Knox RJ, Keen KL, Luchansky L, Terasawa E, Freyer H, Barbee SJ, et al. Comparative effects of sodium pyrithione evoked intracellular calcium elevation in rodent and primate ventral horn motor neurons. Biochemical and biophysical research communications 2008;366(1):48-53.
15. Chen WG, Chang Q, Lin Y, Meissner A, West AE, Griffith EC, et al. Derepression of BDNF transcription involves calcium-dependent phosphorylation of MeCP2. Science 2003;302(5646):885-9.

16. Martinowich K, Hattori D, Wu H, Fouse S, He F, Hu Y, et al. DNA methylation-related chromatin remodeling in activity-dependent BDNF gene regulation. Science 2003;302(5646):890-3.
17. Goto J, Suzuki AZ, Ozaki S, Matsumoto N, Nakamura T, Ebisui E, et al. Two novel 2-aminoethyl diphenylborinate (2-APB) analogues differentially activate and inhibit store-operated Ca(2+) entry via STIM proteins. Cell Calcium 2010;47(1):1-10.
18. Putney JW. Pharmacology of store-operated calcium channels. Mol Interv 2010;10(4):209-18.
19. Gonano LA, Sepulveda M, Rico Y, Kaetzel M, Valverde CA, Dedman J, et al. Calcium-calmodulin kinase II mediates digitalis-induced arrhythmias. Circulation Arrhythmia and electrophysiology 2011;4(6):947-57.
20. Hewavitharana T, Deng X, Wang Y, Ritchie MF, Girish GV, Soboloff J, et al. Location and function of STIM1 in the activation of Ca2+ entry signals. J Biol Chem 2008;283(38):26252-62.
21. Rothberg BS, Wang Y, Gill DL. Orai channel pore properties and gating by STIM: implications from the Orai crystal structure. Sci Signal 2013;6(267):pe9.
22. Soboloff J, Rothberg BS, Madesh M, Gill DL. STIM proteins: dynamic calcium signal transducers. Nat Rev Mol Cell Biol 2012;13(9):549-65.
23. Wang Y, Deng X, Zhou Y, Hendron E, Mancarella S, Ritchie MF, et al. STIM protein coupling in the activation of Orai channels. Proceedings of the National Academy of Sciences of the United States of America 2009;106(18):7391-6.
24. Xiao B, Coste B, Mathur J, Patapoutian A. Temperature-dependent STIM1 activation induces Ca(2)+ influx and modulates gene expression. Nature chemical biology 2011;7(6):351-8.
25. Wang Y, Deng X, Mancarella S, Hendron E, Eguchi S, Soboloff J, et al. The calcium store sensor, STIM1, reciprocally controls Orai and CaV1.2 channels. Science 2010;330(6000):105-9.
26. McNally BA, Somasundaram A, Yamashita M, Prakriya M. Gated regulation of CRAC channel ion selectivity by STIM1. Nature 2012;482(7384):241-5.
27. Li W, Llopis J, Whitney M, Zlokarnik G, Tsien RY. Cell-permeant caged InsP3 ester shows that Ca2+ spike frequency can optimize gene expression. Nature 1998;392(6679):936-41.
28. Zhou Z, Hong EJ, Cohen S, Zhao WN, Ho HY, Schmidt L, et al. Brain-specific phosphorylation of MeCP2 regulates activity-dependent Bdnf transcription, dendritic growth, and spine maturation. Neuron 2006;52(2):255-69.
29. Tao J, Hu K, Chang Q, Wu H, Sherman NE, Martinowich K, et al. Phosphorylation of MeCP2 at Serine 80 regulates its chromatin association and neurological function. Proceedings of the National Academy of Sciences of the United States of America 2009;106(12):4882-7.
30. Gao L, Blair LA, Marshall J. CaMKII-independent effects of KN93 and its inactive analog KN92: reversible inhibition of L-type calcium channels. Biochemical and biophysical research communications 2006;345(4):1606-10.
31. Miyake K, Nagai K. Phosphorylation of methyl-CpG binding protein 2 (MeCP2) regulates the intracellular localization during neuronal cell differentiation. Neurochemistry international 2007;50(1):264-70.

32. Gonzales ML, Adams S, Dunaway KW, LaSalle JM. Phosphorylation of distinct sites in MeCP2 modifies cofactor associations and the dynamics of transcriptional regulation. Molecular and cellular biology 2012;32(14):2894-903.
33. Newman RA, Yang P, Pawlus AD, Block KI. Cardiac glycosides as novel cancer therapeutic agents. Mol Interv 2008;8(1):36-49.
34. Stenkvist B, Bengtsson E, Eriksson O, Holmquist J, Nordin B, Westman-Naeser S. Cardiac glycosides and breast cancer. Lancet 1979;1(8115):563.
35. Prassas I, Paliouras M, Datti A, Diamandis EP. High-throughput screening identifies cardiac glycosides as potent inhibitors of human tissue kallikrein expression: implications for cancer therapies. Clin Cancer Res 2008;14(18):5778-84.
36. Lo-Coco F, Avvisati G, Vignetti M, Thiede C, Orlando SM, Iacobelli S, et al. Retinoic acid and arsenic trioxide for acute promyelocytic leukemia. The New England journal of medicine 2013;369(2):111-21.
37. Grimwade D, Mistry AR, Solomon E, Guidez F. Acute promyelocytic leukemia: a paradigm for differentiation therapy. Cancer Treat Res 2010;145:219-35.
38. Qin T, Si J, Raynal NJ, Wang X, Gharibyan V, Ahmed S, et al. Epigenetic synergy between decitabine and platinum derivatives. Clinical epigenetics 2015;7(1):97.
39. Whitaker M. Calcium at fertilization and in early development. Physiol Rev 2006;86(1):25-88.

Figure Legends

Figure 1. Epigenetic drug screening reveals candidate epigenetic drugs among FDA approved libraries. A, Scheme showing *CMV-GFP* locus in YB5 cells. *CMV* promoter is DNA hypermethylated and marked by repressive chromatin. Epigenetic drugs induced GFP reactivation as shown by GFP fluorescence after decitabine treatment (50 nM, 72h). B, Illustration of dose-schedules selected for drug screening. C, Drug screening results after treatment with library of drugs at 10 μM for 72h. Twenty-three positive hits were identified ($n \geq 1$). D, Drug screening results after treatment with the same library at 50 μM for 24h. Seventy-seven positive hits were identified ($n \geq 1$). E, Venn diagram showing the number of positive hits specific or shared to each dose-schedule and the validation results. F, Positive hits and screening values of GFP expressing cells ($n \geq 1$).

Figure 2. Validation of positive hits with known epigenetic drugs, cardiac glycosides and antibiotics/others subgroups. Dose-response curves were generated measuring GFP expression in a validation step in YB5 cells treated for 24h (left) or 72h (right) with A-B, known epigenetic drugs, C-D, cardiac glycosides and E-F, antibiotics/others ($n \geq 3$).

Figure 3. Gene reactivation by newly identified drugs is independent of DNA demethylation and chromatin modifications. A, *GFP* reactivation in YB5 cells treated for 24h measured by qPCR ($n=3$). B, *SFRP1*, tumor suppressor gene is reactivated after treatment detected by *GFP* fluorescence in HCT116 *SFRP1-GFP* cell line. Cells were treated either 72h with decitabine (followed by 24h without drug) or 24h with the

identified hits at doses indicated on the graph (*n*=3). C, *CMV* promoter and D, *LINE-1* DNA methylation levels measured by bisulfite-pyrosequencing in YB5 cells treated with drugs and doses indicated on the graph (*n*=3). Abbreviations: proscillaridin A (Prosc. A), pyrithion zinc (Pyrith. Z.), cycloheximide (Cyclohex.), and oxyquinoline (Oxyquin.). E, Mass-spectrometry showing histone acetylation levels at several residues in YB5 cells treated for either 72h or 24h with drugs and doses indicated on the graph (*n*=3).

Figure 4. Newly identified drugs induce changes in intracellular Ca^{2+} levels. Intracellular changes in Ca^{2+} levels in YB5 cells pretreated for 8h with A, known epigenetic drugs, B, cardiac glycosides, C, pyrithion zinc and disulfiram, in response to ionomycin, extracellular Ca^{2+} and thapsigargin. D, Time-lapse intracellular Ca^{2+} changes in HEK293 cells overexpressing STIM1-Orai1 proteins pretreated for 8h with digitoxin in response to ionomycin and extracellular Ca^{2+}. Time-lapse intracellular Ca^{2+} changes in HEK293 cells transfected with E, constitutively active STIM1 mutant protein (D67A) or with F, constitutively active Orai mutant channel (V102C) in response to extracellular Ca^{2+} exposure and SOCe inhibitor (2-APB). The arrows indicate the addition of Ca^{2+} into the extracellular media while a line indicate the time of Ca^{2+} exposure prior its removal by washes of Ca^{2+} free-solution. Fexofenadine was used as a control since this drug does not induce GFP reactivation.

Figure 5. Drug-induced gene reactivation is dependent on CamK activity. A, GFP reactivation by flow cytometry in YB5 cells pretreated (4h) with CamK inhibitor Kn-93

and its weaker analog Kn-92 and treated for 24h. B, Fluorescent immunochemistry in SW48 cells (YB5 parental cells) treated for 24h and 48h with proscillaridin at 500 nM stained with DAPI, MeCP2 (RFP) antibody. White arrows show MeCP2 signal in the cytoplasm post-proscillaridin A treatment. C, Percentage of apoptotic cells in YB5 cells pretreated (4h) with CamK inhibition and treated for 48h.

Figure 6. Anticancer efficacy and selectivity of candidate epigenetic drugs. Anchorage-dependent toxicity assays were performed in YB5 cells treated for 72h (top) or 24h (bottom) with A, know epigenetic drugs, B, cardiac glycosides, and C, antibiotics/others (Abbreviations: Pyrition zinc: Pyrithion; Oxiquinoline: Oxiquin.; Cycloheximide: Cyclohex.) (*n*=3). D, Anchorage-independent clonogenic assays in soft agar were performed after a 24h treatment at the doses indicated on the graph (*n*=3). E, Cell viability assays using normal colon cells (CRL-1831) and SW48 (YB5's parental cell line) after a 48h treatment measured by flow cytometry. Drugs and doses are indicated on the graph (*n*=3).

Author Manuscript Published OnlineFirst on December 30, 2015; DOI: 10.1158/0008-5472.CAN-14-2391
Author manuscripts have been peer reviewed and accepted for publication but have not yet been edited.

Figure 1

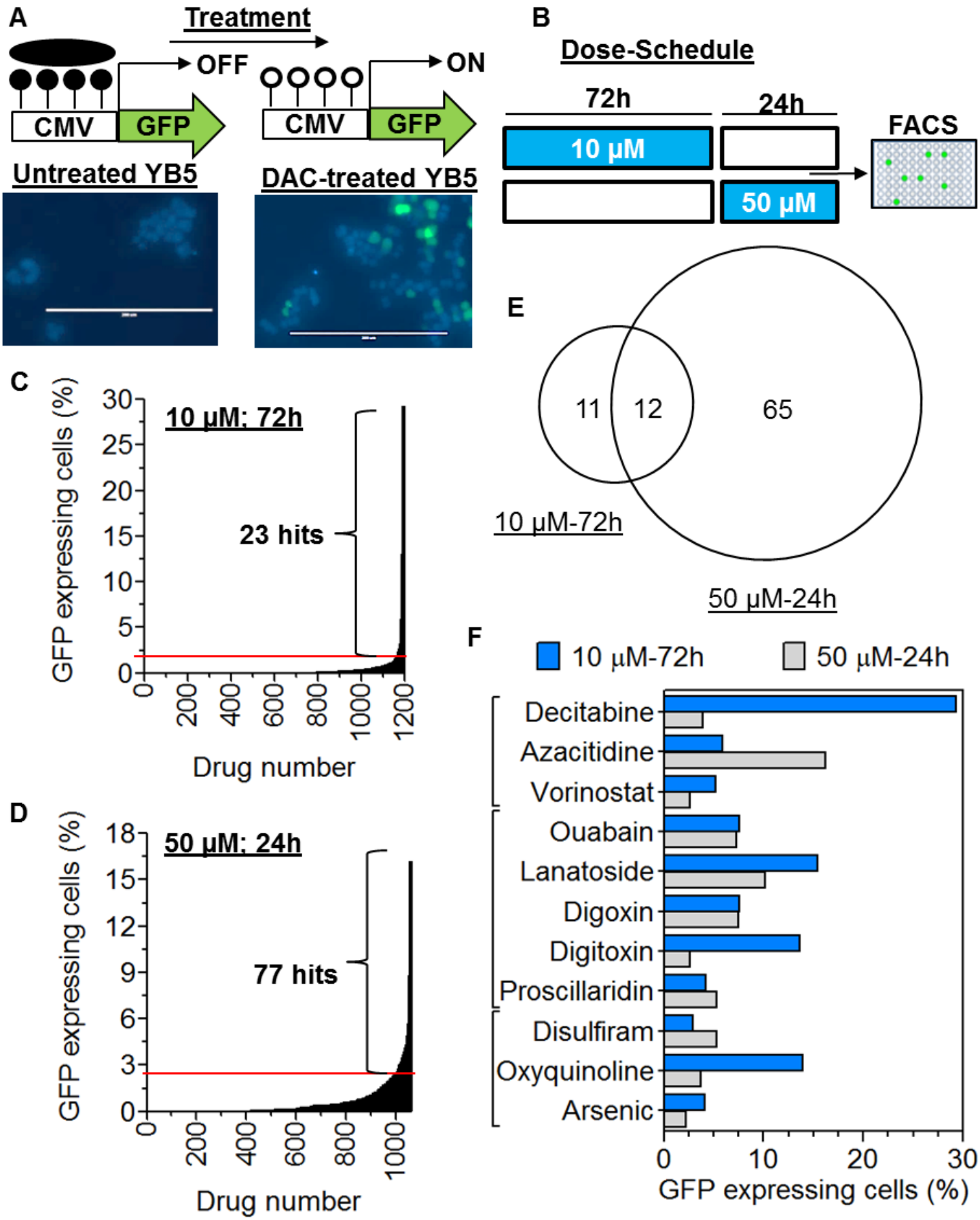

Author Manuscript Published OnlineFirst on December 30, 2015; DOI: 10.1158/0008-5472.CAN-14-2391
Author manuscripts have been peer reviewed and accepted for publication but have not yet been edited.

Figure 2

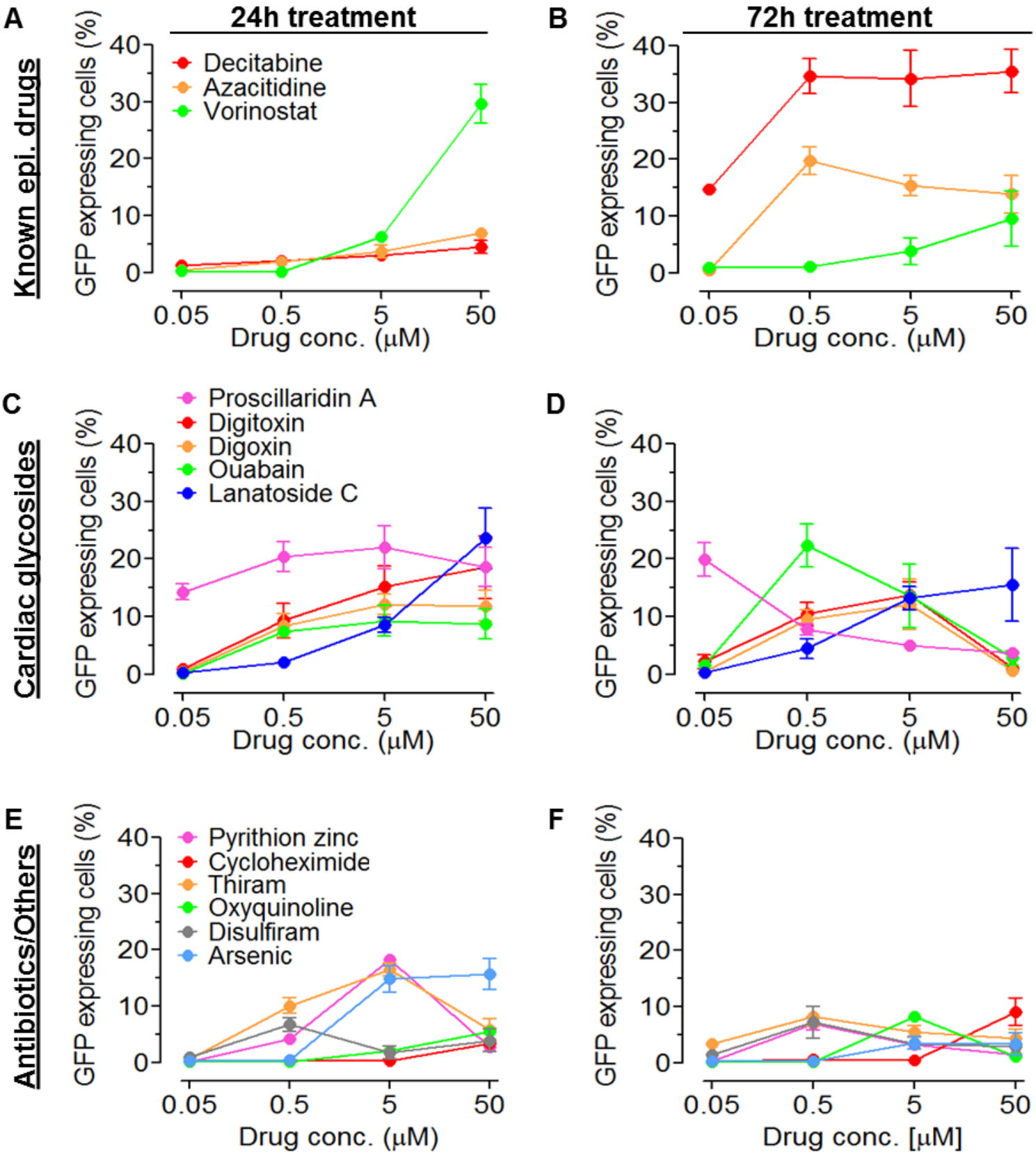

Figure 3

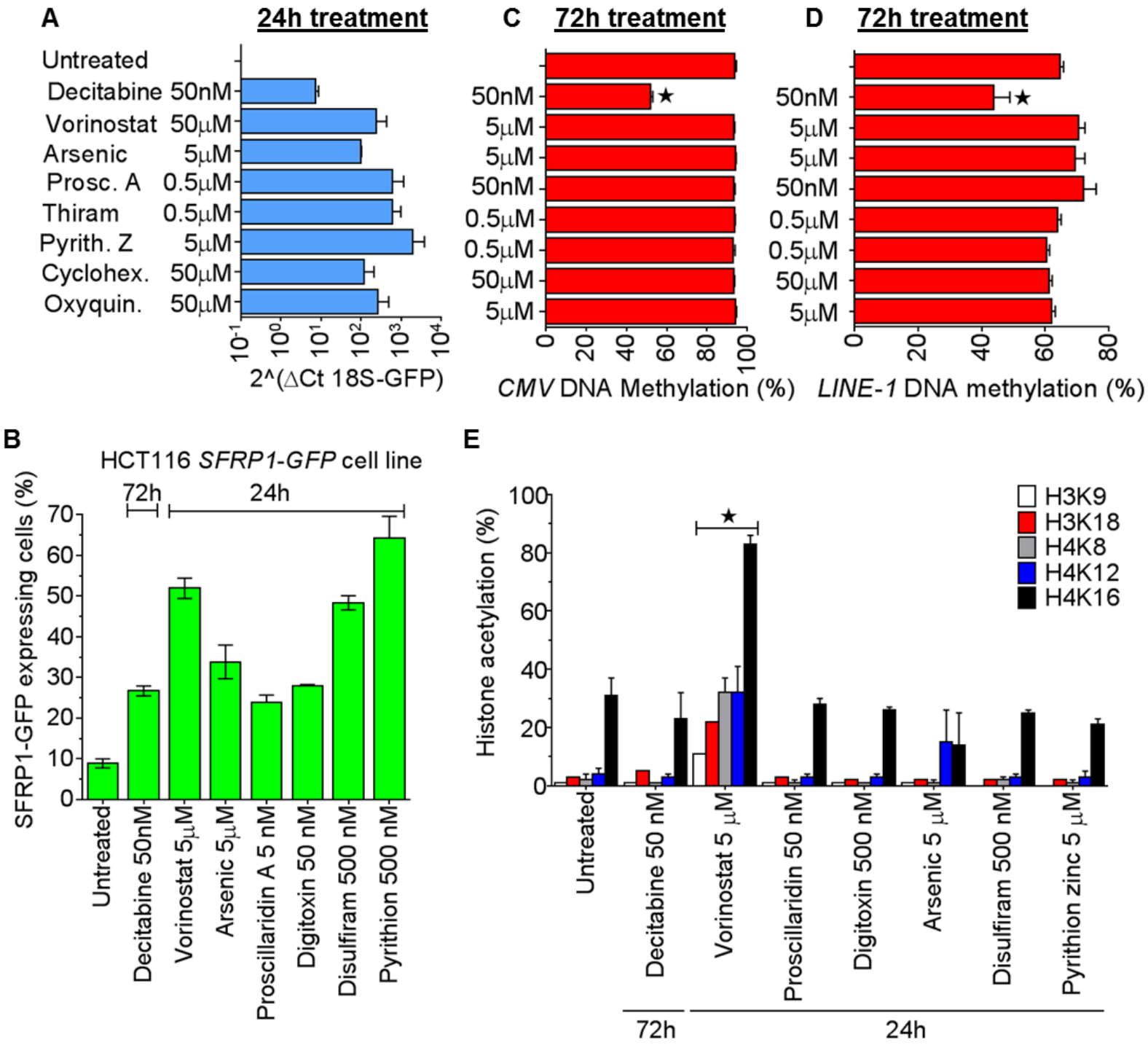

Author Manuscript Published OnlineFirst on December 30, 2015; DOI: 10.1158/0008-5472.CAN-14-2391
Author manuscripts have been peer reviewed and accepted for publication but have not yet been edited.

Figure 4

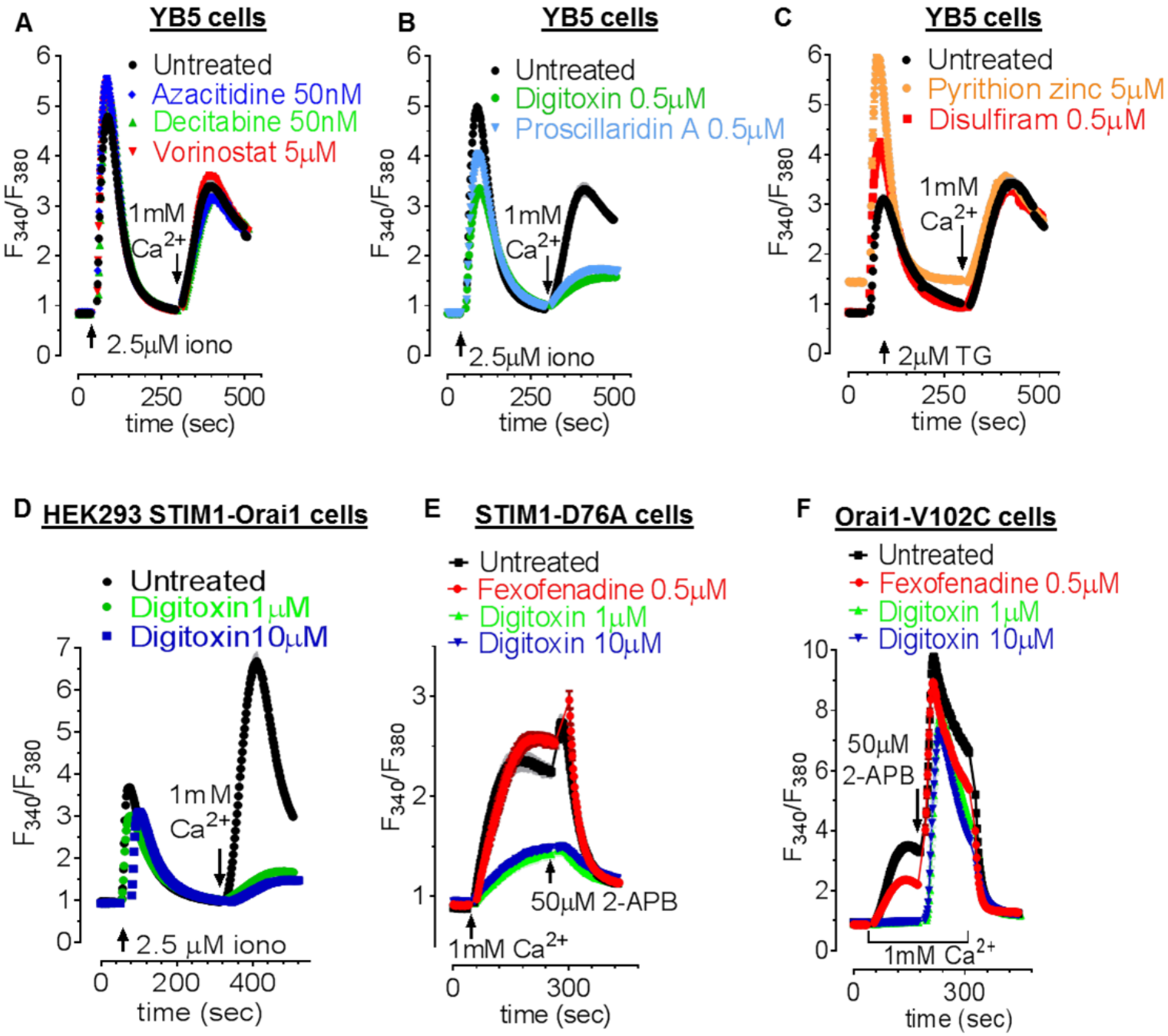

Figure 5

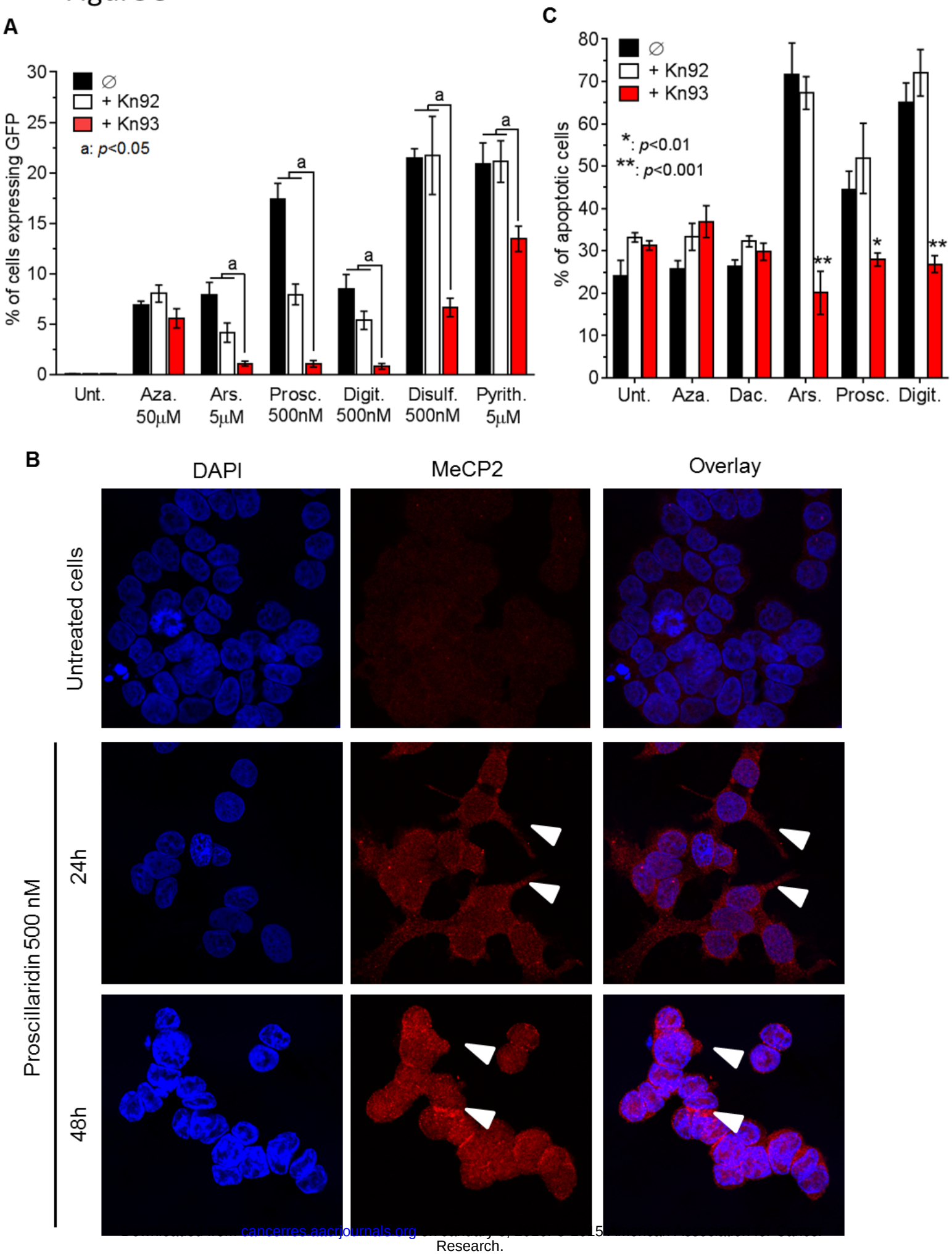

Figure 6

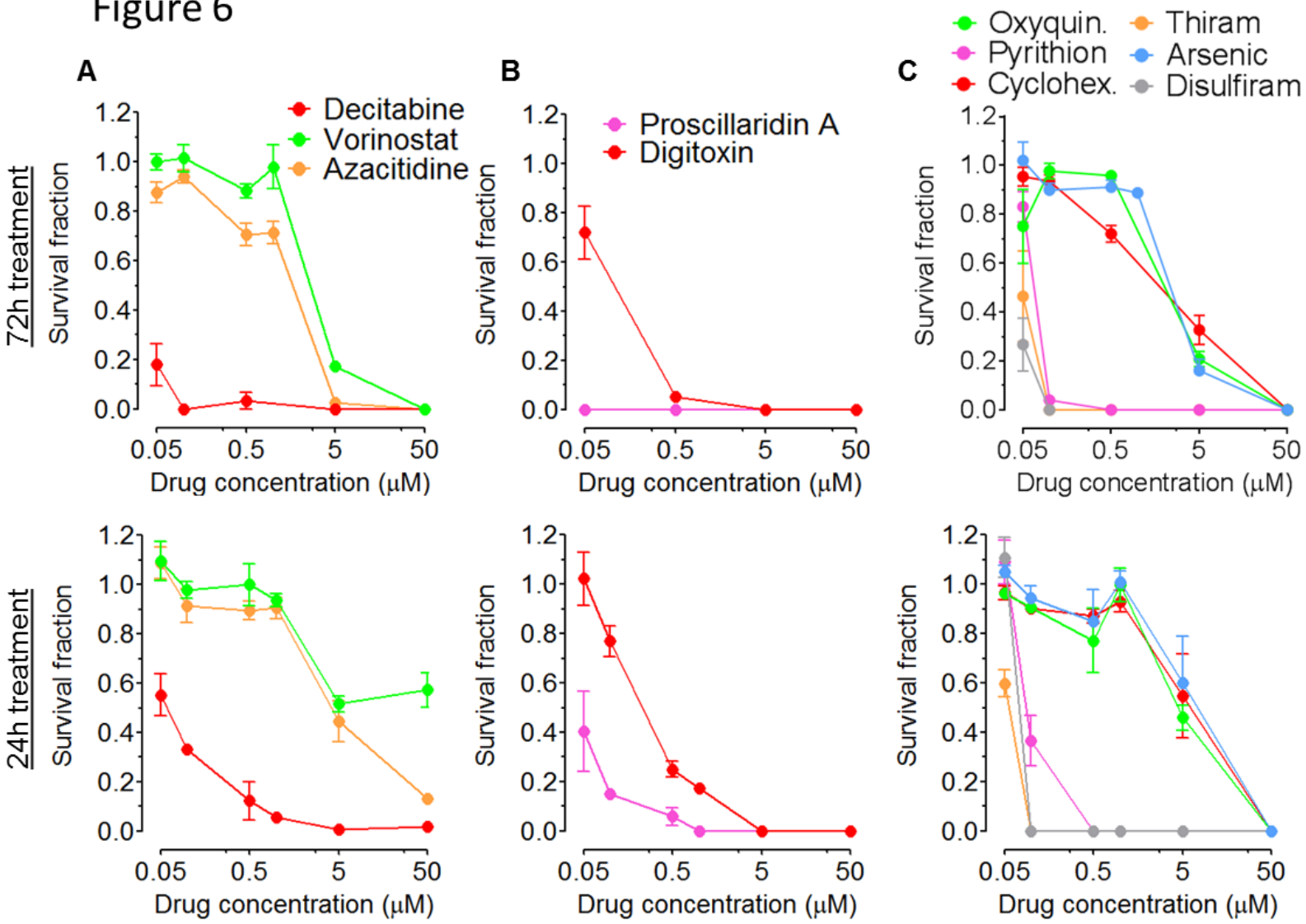

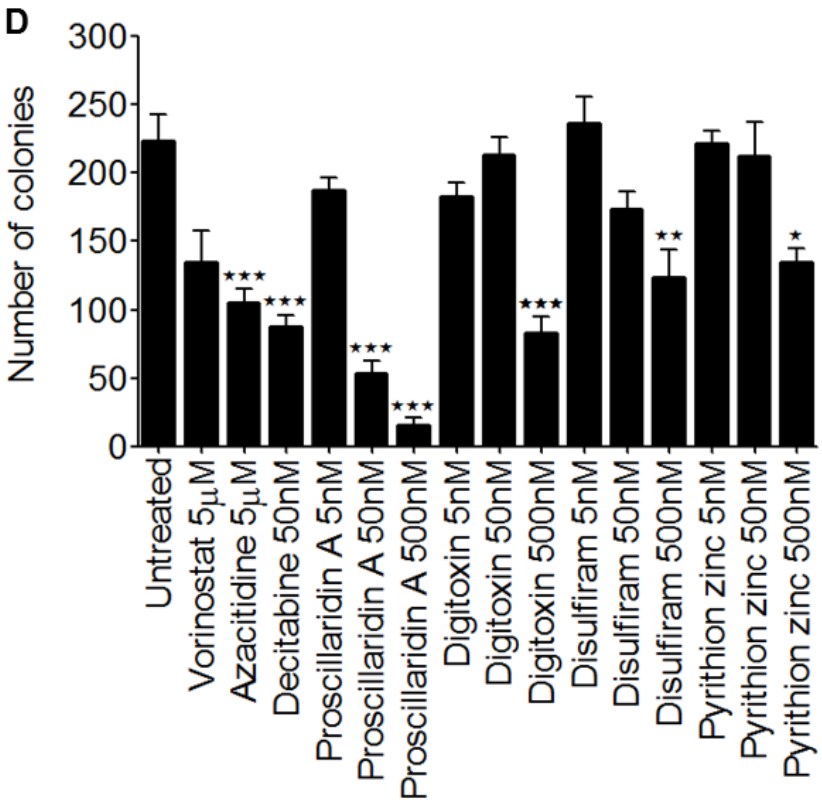

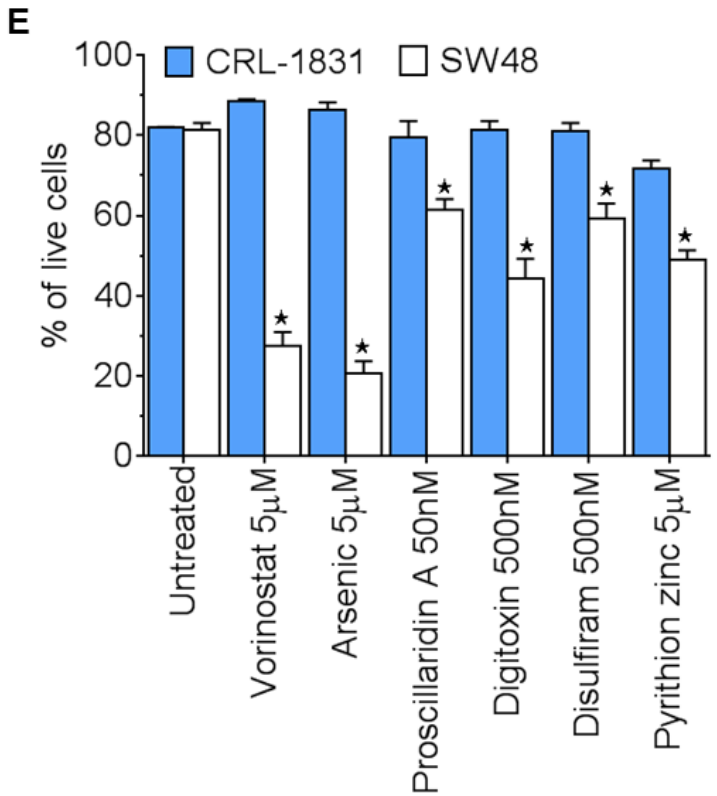

AACR American Association for Cancer Research

Cancer Research

The Journal of Cancer Research (1916–1930) | The American Journal of Cancer (1931–1940)

Targeting calcium signaling induces epigenetic reactivation of tumor suppressor genes in cancer

Noel J-M Raynal, Justin T. Lee, Youjun Wang, et al.

Cancer Res Published OnlineFirst December 30, 2015.